Modelling pathogen fate in stormwaters by a particle–pathogen interaction model using population balances

L. Vergeynst, B. Vallet and P. A. Vanrolleghem

ABSTRACT

Stormwater is polluted by various contaminants affecting the quality of receiving water bodies. Pathogens are one of these contaminants, which have a critical effect on water use in rivers. Increasing the retention time of water in stormwater basins can lead to reduced loads of pathogens released to the rivers. In this paper a model describing the behaviour of pathogens in stormwater basins is presented including different fate processes such as decay, adsorption/ desorption, settling and solar disinfection. By considering the settling velocity distribution of particles and a layered approach, this model is able to create a light intensity, and particle and pathogen concentration profile along the water depth in the basin. A strong effect of solar disinfection is discerned. The model has been used to evaluate pathogen removal efficiencies in stormwater basins. It includes a population of particle classes characterized by a distribution of settling velocities in order to be able to reproduce stormwater quality and treatment in a realistic way.

Key words | disinfection, Gujer matrix, population balance modelling, sedimentation stormwater management

L. Vergeynst
B. Vallet
P. A. Vanrolleghem (corresponding author)
modelEAU,
Département de génie civil et de génie des eaux,
Université Laval,
1065 av. de la Médecine,
Québec, Qc,
Canada G1V 0A6
E-mail: Peter.Vanrolleghem@gci.ulaval.ca

INTRODUCTION

For decades it has been known that stormwater can cause severe flooding problems in urban areas and also affects the receiving water's quality as it contains a considerable amount of suspended solids and pollutants associated with them (trace metals, pathogens…) (Pettersson 2002; Vaze & Chiew 2004; Characklis et al. 2005). To reduce flooding problems, stormwater basins have been built in new urban developments. The present study is a part of a larger project in which a new approach is developed to augment these existing infrastructures with an operational strategy that improves the eco-hydraulics of the receiving water body into which it eventually discharges the retained stormwater (Muschalla et al. 2009). The idea behind the strategy is to operate a sluice gate at the outlet of a stormwater basin on the basis of a set of rules to enhance the removal efficiency of, especially, fine particles by increasing the retention time of stored stormwater. The contribution of the work presented here is a dynamic model that can support evaluating the efficiency of control rules in terms of the

expected reduction of the load of pathogens discharged into the river.

Escherichia coli (*E. coli*) in stormwater is found in concentrations between 10^2 and 10^4 CFU (colony forming units)/100 mL, 20 to 50% of which are attached to suspended solids (Characklis et al. 2005; Jeng et al. 2005; Krometis et al. 2007). The other bacteria are free floating and present as free bacteria or in aggregates. The degree to which pathogens are attached to particles influences their transport and decay. Adsorption of pathogens to particles followed by sedimentation is an important mechanism for removal of pathogens from the bulk liquid that will eventually be discharged. The sedimentation velocity of particles and the distribution of pathogens to these particles determine the pathogen sedimentation efficiency. Jeng et al. (2005) and Oliver et al. (2007) found that more than 90% of attached pathogens are associated with particles smaller than 30 μm in stormwater. Besides, the extent, strength and nature of pathogen–particle adsorption is influenced

by the particle surface characteristics. Organic, clay and silt suspended matter tend to attach more pathogens than sand because the surface area to volume ratio is higher for smaller particles (Guber *et al.* 2007). Additionally, the greater surface charge on organic, clay and silt suspended matter enhance the sorption process (Hipsey *et al.* 2006). According to Stokes' law, the smaller and lighter (organic) particles decant slowly and thus slow down the pathogen sedimentation process. Garcia-Armisen & Servais (2009) observed settling rates of particle-associated *E. coli* in river water between 0 (no suspended matter) and 1.6 m d^{-1}.

Decay of pathogens is a second important removal mechanism. Struck *et al.* (2008) predicted the pathogen concentration in retention ponds and constructed wetlands for stormwater and applied a first-order decay function that includes natural decay with temperature correction, predation, solar disinfection and a term that includes sorption, filtration and sedimentation. Natural decay is subject to many environmental conditions such as conductivity, dissolved oxygen, oxygen reduction potential, pH, salinity, etc. Solar radiation causes notable pathogen decay, especially in shallow waters (Curtis *et al.* 1992). The pathogen–particle interaction is also important in the sense that pathogens tend to survive longer when attached to particles (Struck *et al.* 2008), for instance by the shielding from solar radiation and protection from predation, thus lowering the disinfection rate of attached bacteria.

MATERIALS AND METHODS

Model description

As mentioned above, an important *E. coli* removal mechanism is through sedimentation of the particles to which they are attached. The model presented in this paper is an extension of the more general stormwater sedimentation model of Vallet *et al.* (2011) developed in the aforementioned overall project. The Vallet model allows reproduction of the particle concentration gradient and the behaviour of pollutants associated with them. To describe the vertical spatial heterogeneity it uses the layer approach adopted in wastewater treatment settler models (Vitasovic 1989) around which a mass balance is built for both water and pollutants. In this model a population of particle classes is defined. For each class a different sedimentation velocity v_k (m d^{-1}) is defined with an associated suspended solids mass X_k ($k = 1$, NrOfClasses).

In order to experimentally determine the fraction of each of the classes, the ViCA protocol (Chebbo & Grommaire 2009) was used. The protocol applies a sedimentation column in which, during successive increasing predefined time intervals (e.g. 0 to 1 min, 1 to 2 min, 2 to 4 min, 4 to 8 min, etc.) the settled solids are recovered at the bottom of the column in different aluminium cups. In each cup the particle mass settled is composed of particles with high settling velocity coming from the top of the column and particles with a lower settling velocity coming from a lower part of the column. Therefore, a mathematical treatment of the cumulative settled mass (sum of the masses of the different classes in each cup) versus time enables calculation of the fractions of each velocity class (Chebbo & Grommaire 2009). These experiments have proven to be an efficient tool to support the model used in the present paper (Vallet *et al.* 2010). The information collected from ViCA settling experiments can also be used to support a pathogen population balance model. Given the sedimentation velocities and the mass balance for each particle class, the population balance model therefore allows simulation of the dynamics of the particles and attached pathogens along the depth of the stormwater basin. As illustration of the particle–pathogen interaction model is the major focus of the paper, the mass balance of each layer in the stormwater basin is derived from Vallet *et al.* (2010), considering only sedimentation and no advection or mixing transport processes of suspended solids and their associated pathogens:

$$\frac{dX_{k_i}}{dt} = -A \cdot v_k \cdot X_{k_i} + A \cdot v_k \cdot X_{k_{i-1}}$$
$$+ conversions_i \quad (k = 1, \text{NrOfClasses})$$

where X_{k_i} is the concentration of the kth particle class in the ith layer (g m^{-3}); the top layer of the stormwater basin is layer 1; the sediment layer is layer 10; A is the surface area of the stormwater basin (m^2). The first part of the mass balance accounts for particles settling out of layer i into layer $i + 1$ and has a negative sign. Particles settling out of the $i - 1$th layer increase the concentration in the ith layer in the second part of the mass balance. Straightforwardly, there are no particles settling into the top layer and no particles can settle out of the bottom layer. For components in solution, i.e. free pathogens, no sedimentation occurs and so the mass balance is reduced to their conversion processes:

$$\frac{dS_i}{dt} = conversions_i$$

Decay, disinfection, (de)sorption and growth processes are grouped in the conversion term, which is discussed below.

Process description

To each of the described particle classes, pathogens can sorb/desorb and their population balance allows calculation of the concentration of particle-associated pathogens in each layer. Sorption and desorption of pathogens to particles is described by isotherms of the sorption/desorption equilibrium which, for low concentrations, are based on a linear partition coefficient, K_D ($m^3\,g^{-1}$). Sorption and desorption are two oppositely directed processes with the following respective rates:

$$rate\ of\ sorption = k_{sorption} \cdot S_{path} \cdot X$$

and

$$rate\ of\ desorption = k_{desorption} \cdot X_{path}$$

where $k_{sorption}$ and $k_{desorption}$ ($m^3\,g^{-1}\,d^{-1}$) are respectively the sorption and desorption rate coefficients (Jacobsen & Arvin 1996; Lindblom et al. 2006); X is the particle concentration of a particle class ($g\,m^{-3}$); S_{path} is the concentration of 'free' E. coli (pathogens m^{-3}); and X_{path} is the

concentration of attached E. coli (pathogens m^{-3}). The overall sorption/desorption process rate for each particle class is presented in Table 1 and includes the partition coefficient, K_D, which is equal to the ratio of the desorption to the sorption rate coefficients.

Inactivation of E. coli in stormwater basins is principally described by three mechanisms: (a) natural decay, (b) predation and (c) solar disinfection. These processes have been implemented for both particulate and free E. coli populations. Predation is often incorporated in the natural decay term because of the difficulty in measuring this separately (Struck et al. 2008). In the proposed model, the combination of predation and natural decay is called 'base decay'. Base decay of free pathogens and particle-associated pathogens is described by a first-order base mortality plus a term that includes mortality due to salinity. The whole base decay is corrected for temperature, which is considered constant over depth in a shallow stormwater basin (Mancini 1978). Solar disinfection depends on light intensity, which decreases with increasing depth due to turbidity (light extinction according to Beer's law), another, albeit indirect, particle–pathogen interaction. In addition, at a certain depth, all free pathogens and a distinct fraction of particle-associated pathogens ($F_{I,X_{path}}$) are assumed to be equally influenced by solar radiation, whereas the remaining fraction of the particle-associated pathogens is

Table 1 | Gujer matrix representation of the population particle–pathogen interaction model

Process	State variables S_{path}	X_1	X_2	$X_{path,1}$	$X_{path,2}$	Process rate
Growth of S_{path}	+1					$\mu_{S_{path}} \cdot S_{path}$
Base decay of S_{path}	−1					$((b_{S_{path}} + k_{salt,path} \cdot S_{salt}) \cdot \theta_{T_{20,path}}^{T-20})S_{path}$
Disinfection of S_{path}	−1					$\alpha_{I,path} \cdot I \cdot S_{path}$
Growth of $X_{path,1}$				+1		$\mu_{X_{path,1}} \cdot X_{path,1}$
Growth of $X_{path,2}$					+1	$\mu_{X_{path,2}} \cdot X_{path,2}$
Base decay of $X_{path,1}$				−1		$((b_{X_{path,1}} + k_{salt,path} \cdot S_{salt}) \cdot \theta_{T_{20,path}}^{T-20})X_{path,1}$
Base decay of $X_{path,2}$					−1	$((b_{X_{path,2}} + k_{salt,path} \cdot S_{salt}) \cdot \theta_{T_{20,path}}^{T-20})X_{path,2}$
Disinfection of $X_{path,1}$				$-F_{I,X_{path,1}}$		$\alpha_{I,path} \cdot I \cdot X_{path,1}$
Disinfection of $X_{path,2}$					$-F_{I,X_{path,2}}$	$\alpha_{I,path} \cdot I \cdot X_{path,2}$
Sorption of S_{path} on $X_{path,1}$	−1			+1		$k_{sorption,1} \cdot \left(S_{path} \cdot X_1 - \dfrac{X_{path,1}}{K_{D_1}} \right)$
Sorption of S_{path} on $X_{path,2}$	−1				+1	$k_{sorption,2} \cdot \left(S_{path} \cdot X_2 - \dfrac{X_{path,2}}{K_{D_2}} \right)$

$\mu_{S_{path}}$: growth rate of free pathogens (d^{-1}); $\alpha_{I,path}$: proportionality constant for influence of light ($m^2\,W^{-1}\,d^{-1}$).
$b_{S_{path}}$: decay rate of free pathogens (d^{-1}); $\mu_{X_{path,1\,reps.\,2}}$: growth rate of pathogens adsorbed on respectively X_1 and X_2 (d^{-1}).
$k_{salt,path}$: salinity influence factor ($d^{-1}\,ppt^{-1}$); $b_{X_{path,1\,resp.\,2}}$: decay rate of pathogens adsorbed on respectively X_1 and X_2 (d^{-1}).
$\theta_{T_{20},path}$: temperature coefficient (–); $k_{sorption,1\,resp.\,2}$: sorption rate coefficient for pathogens adsorbed on respectively X_1 and X_2 ($m^3\,g^{-1}\,d^{-1}$).
S_{salt}: salt concentration (ppt); $F_{I,X_{path,1\,resp.\,2}}$: fraction of pathogens adsorbed on respectively X_1 and X_2 exposed to light (–).
T: temperature (°C); $K_{D_{1\,resp.\,2}}$: sorption equilibrium coefficient for pathogens adsorbed on respectively X_1 and X_2 ($m^3\,g^{-1}$).
I: solar radiation intensity ($W\,m^{-2}$).

protected from solar radiation by shielding (Fenner & Komvuschara 2005). A first-order mortality constant for solar disinfection, proportional to light intensity, is applied (Chapra 1997; Struck *et al.* 2008). Growth of *E. coli*, while not expected in stormwater basins, is also included for generality and use in, for instance, combined sewer system models.

The average solar radiation intensity, I_i (W m^{-2}), over each layer is calculated according to Chapra (1997) where I_{0_i} (W m^{-2}) is the radiation intensity at the top of each layer derived from Beer's law:

$$I_i = \frac{I_{0_i}}{K_{e_i} \cdot H_i} \cdot (1 - e^{K_{e_i} \cdot H_i})$$

$$I_{0_i} = (1 - F_{I,\alpha}) \cdot I_{surface} \cdot e^{-\sum_{l=1}^{l=i-1} Ke_l \cdot H_l}$$

where $I_{surface}$ is the incoming solar radiation intensity (w m^{-2}); H_i is the height of layer i (m); the term $(1-F_{I,a})$ accounts for the fraction of the incoming light penetrating the water surface (–). The global extinction coefficient over the ith layer, K_{e_i} (m^{-1}), increases linearly with the total suspended solid (TSS) concentration (mg L^{-1}) added to a constant extinction coefficient due to water, $K_{e,water}$:

$$K_{e_i} = K_{e,X} \cdot TSS_i + K_{e,water}$$

Note that the population balance over the particle classes allows calculation of the TSS concentration (g m^{-3}) in each of the layers:

$$TSS_i = \sum_{k=1}^{NrOfClasses} X_{k_i}$$

Finally to represent the diurnal variation of the light intensity, $I_{surface}$ is described by the following equation:

$$I_{surface} = \max\left(\frac{I_{max}}{3} + \frac{2 \cdot I_{max}}{3} \cdot \sin\left(\frac{3\pi}{2} + 2\pi \cdot t\right); 0\right)$$

where I_{max} is the maximum light intensity during the day period (W m^{-2}). This equation allows the reaching I_{max} at noon with a sinusoidal pattern for the rest of the day and a zero value during the night.

Gujer matrix presentation

Also originating from wastewater treatment modelling, the Gujer matrix approach to present the physico-chemical and biological processes in a system (previously known as Petersen matrix, (Henze *et al.* 1987)), is adopted here to concisely present the previous discussed decay, disinfection, (de)sorption and growth equations. Table 1 represents the Gujer matrix for a system with two particle classes (NrOfClasses = 2), but it can be observed that it is easy to augment the matrix for a larger number of classes. In the Gujer matrix, the overall conversion equation for each state variable can be obtained by summating the products of the process coefficients and the corresponding process rates. Please note as well that in this matrix no reference is given to the layer in the stormwater basin to which it applies. In fact the mass balance of each layer contains such a Gujer matrix to calculate the conversion processes taking place, next to the transport processes. Again, augmenting the stormwater basin model with more layers is straightforward.

Model implementation and simulations

The model has been implemented in the WEST modelling and simulation software (MIKE by DHI software, Hørsholm, Denmark), which is used for wastewater treatment plant modelling and integrated urban wastewater system modelling (Vanhooren *et al.* 2003). The WEST model base is written in a user-friendly Model Specification Language (MSL) which is a declarative language presenting only the model equations. The WEST compiler is capable of programming the solution of the model from the MSL code. The particle–pathogen interaction model was implemented as an extension of the more general sedimentation model of Vallet *et al.* (2010) by adopting the Gujer matrix editor provided in WEST for the description of the particle–pathogen interaction processes. The Vallet model and the light extinction equations were implemented using respectively ordinary differential and algebraic equations.

SIMULATION RESULTS AND DISCUSSION

In order to illustrate the pathogen dynamics induced by the different processes involved in the model and the effect of a heterogeneous suspension of particles, two specific simulations have been run with respectively a single and three particle classes. The initial concentrations have been set to 10^3/100 mL for free *E. coli*, 0 for particle-associated *E. coli* and 75 mg L^{-1} for TSS (average concentration observed during sampling campaign (Carpenter *et al.* 2011)). In the first simulation, the particle–pathogen interactions for only one particle class are simulated. The settling velocity of

$1 \, \text{m} \, \text{d}^{-1}$ is chosen to emphasize the different particle–pathogen interaction processes. The partition coefficient is calculated so that at sorption equilibrium 38% of the pathogens is adsorbed to the suspended matter at a TSS concentration of $75 \, \text{mg} \, \text{L}^{-1}$ (Vergeynst 2010). In previous work by Vallet et al. (2011), the number of particle classes, their corresponding mass fractions and sedimentation velocities were optimized for the conditions encountered during the sampling campaign. Three particle classes with a sedimentation velocity of 0.1, 2 and $80 \, \text{m} \, \text{d}^{-1}$ were found to be sufficient to represent the particle dynamics in the stormwater basin. These conditions are used to conduct the second simulation. The distribution coefficients are calculated based on the same sorption equilibrium as in the first simulation and such that the distribution coefficients are the same for the two slowest settling particle classes and a factor of ten lower for the third particle class. Based on a literature study, Vergeynst (2010) suggested that for clay and silt size suspended solids (slow settling particles) the attached pathogens to particle mass ratio is more or less constant whereas the ratio is roughly ten times smaller for sand size suspended solids (fast settling particles). The particle specific parameters are presented in Table 2. The other parameters in Table 3 are the same for each of the classes and have been taken from the literature. Finally, the light intensity has been chosen for a typical summer day in Québec, considering the maximum value as the double of the average referred to by Natural Resources Canada (2010). Simulations were run with a water height of 1 m represented by ten layers of equal height. The first layer is the top layer of the stormwater basin, the ninth layer is the bottom layer and the tenth layer the sediment layer where settled suspended matter accumulates. The duration has been set to four days in order to see the effect of diurnal variation of the light and not to exceed the maximum residence time of stormwater as defined in the overall project (Muschalla et al. 2009). A Runge–Kutta 4 numerical integration with a variable time-step was applied as provided by the modelling software.

First, the simulation results for a single particle class are discussed. Subsequently the simulation results with three particle classes are discussed and compared with the first simulation results. Figure 1 presents the results of the first simulation with a single particle class. The solar radiation intensity (a), attached (b), and free *E. coli* concentration (c) are shown for the surface layer (L1, 0 to 0.1 m deep), an intermediate layer (L5, 0.4 to 0.5 m deep), the bottom layer (L9, 0.8 to 0.9 m deep) and the sediment layer (L10).

Table 3 | General parameter values used for simulations

| Symbol	Description	Value	Unit
$b_{S_{path}}$	decay rate of free pathogens	0.8^a	d^{-1}
$b_{X_{path}}$	decay rate of pathogens adsorbed on X	0.4^b	d^{-1}
$k_{salt.path}$	salinity influence factor	0.02^a	$\text{d}^{-1} \, \text{ppt}^{-1}$
$\theta_{T_{20}.path}$	temperature dependency coefficient	1.013^c	–
$\mu_{S_{path}}$	growth rate of free pathogens	0^b	d^{-1}
$\mu_{X_{path}}$	growth rate of pathogens adsorbed on X	0^b	d^{-1}
$\alpha_{I.path}$	proportionality constant for influence of light	0.006^c	$\text{m}^2 \, \text{W}^{-1} \, \text{d}^{-1}$
$F_{I,X_{path}}$	fraction of pathogens adsorbed on X exposed to light	0.95^b	–
$k_{sorption}$	sorption rate coefficient of free pathogens on X	0.58^b	$\text{m}^3 \, \text{g}^{-1} \, \text{d}^{-1}$
I_{max}	maximum light intensity during the day	480	$\text{W} \, \text{m}^{-2}$
$F_{I,\alpha}$	light reflection factor at the surface of water	0.28^b	–
$K_{e,X}$	extinction coefficient due to TSS	0.55^a	$\text{m}^2 \, \text{g}^{-1}$
$K_{e,water}$	extinction coefficient due to water colour	0.05^c	m^{-1}
T	temperature	15^b	$°\text{C}$
S_{salt}	salt concentration	$0,1^b$	ppt

[a]Chapra (1997).
[b]Vergeynst (2010).
[c]Struck et al. (2008).

Table 2 | Particle specific parameter values used for simulations

Symbol	Description / Particle class	1 Part. class X	3 Part. classes X_1	X_2	X_3	Unit
	mass fraction of X_k	1	0.33	0.65	0.12	–
v_k	sedimentation velocity of X_k	1	80	2	0.1	$\text{m} \, \text{d}^{-1}$
K_{D_k}	partition coefficient for pathogens adsorbed on X_k	0.0081	0.00115	0.0115	0.0115	$\text{m}^3 \, \text{g}^{-1}$
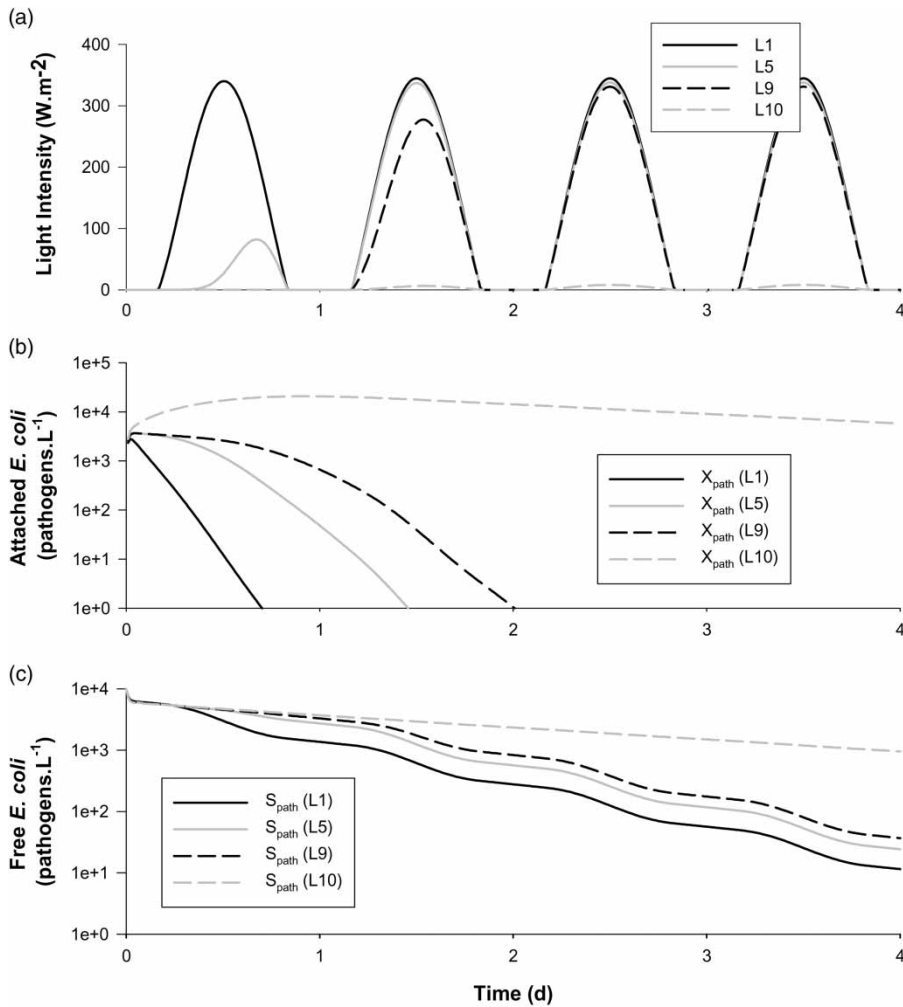
Figure 1 │ Simulation results considering a single particle class with a settling velocity of 1 m d^{-1}. Parameters shown are light intensity (a), attached (b) and free (c) *E. coli* for layers 1, 5, 9 and 10.

Single particle class results

The light intensity is following a sinusoidal pattern from sunrise to sunset. The intensity is maximal at the surface and decreases gradually with the depth reaching almost a zero value in the sediment layer. Along the four days of simulation the light intensity below the surface increases as the suspended solids settle out. This increase in light intensity is slower in deeper layers due to the larger distance for particles to settle. After four days, the light intensities at the surface (L1) down to the bottom (L9) are almost superimposed, meaning that maximal light intensity in all layers is attained when all particles are settled out (Figure 1(a)). The small remaining difference in intensity between the surface and subsurface layers is due to the extinction caused by the water itself. Notice

that the light never reaches the sediment layer (L10) where sediment accumulates.

Instantly, the attached and free bacteria fractions reach sorption equilibrium with 38% of the total *E. coli* being attached to particles. Then, the attached pathogens settle with the particles (Figure 1(b)). The attached *E. coli* concentration at the bottom of the basin (Figure 1(b), X_{path} (L10)) increases during the first two days because of the accumulation of settled particles with attached bacteria, but then decay takes over.

The removal of free *E. coli* (Figure 1(c)) increases as the particulate concentration decreases, which leads to increasing solar disinfection. Without radiation, at night, the removal of free pathogens is only caused by base decay. The steeper decrease during daytime is caused by the effect of solar disinfection. This phenomenon is visible in

the stepwise shape of the decreasing concentration profiles. This increase in solar disinfection takes longer to occur in the deeper layers because the particles take longer to settle out, leading to lower light intensities. At the surface (L1), solar disinfection can be observed from the first day whereas at the bottom (L9) it takes more than two days to see the effect of solar disinfection. The importance of the solar disinfection in this model can be concluded from the decrease of free bacteria in the deeper layers. As soon as the particles are settled out and a higher light intensity reaches subsurface layers (during the second day), the pathogen concentration begins to decrease faster than under simple decay, as occurred in the sediment layer (L10).

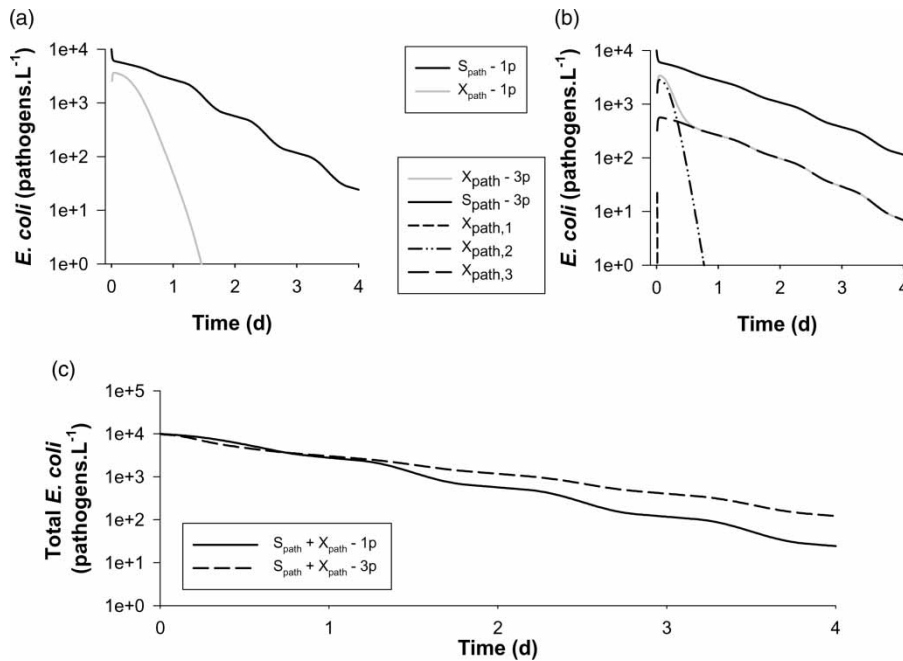## Comparison of 1 and 3 particle class models

Figures 2 and 3 present the results in layer 5 for the simulation with a single and three particle classes. The results for the single particle class are extracted from Figure 1 and compared to the results for three particle classes to emphasize the effect of a heterogeneous suspension of particles on the particle–pathogen interactions in a more realistic description of the stormwater composition.

Figure 2 presents the TSS concentration in layer 5 of both simulations (a) and three particle class (b) model in the layers 1, 5 and 9. On Figure 2(a) the successive settling of the three particle classes can be seen. The TSS concentration drops at the start of the simulation by 33% due to the settling of X_1, the fastest settling particle class. After that, the TSS concentration decreases due to the second particle class (X_2) settling out down to a remaining 11% of the initial TSS concentration. For a more detailed discussion of the modelling of heterogeneous suspension of particles, the reader is referred to Vallet *et al.* (2011). In the simulation with a single particle class (Figure 1(a)) light intensity in layer 5 is maximal in the fourth day whereas in the simulation with three particle classes, light intensity only reaches 54% of the maximal light intensity (Figure 2(b)). This difference is caused by the higher remaining TSS concentration in the subsurface layers. Here, 6% of total TSS (mainly composed of X_3) is still remaining in suspension at the end of the simulation. Although the TSS concentration is low, the light penetration is still highly affected, which can be explained by the exponential function in the light extinction equation.

In Figure 3 the free and attached *E. coli* concentration in layer 5 are presented for respectively a single (a) and
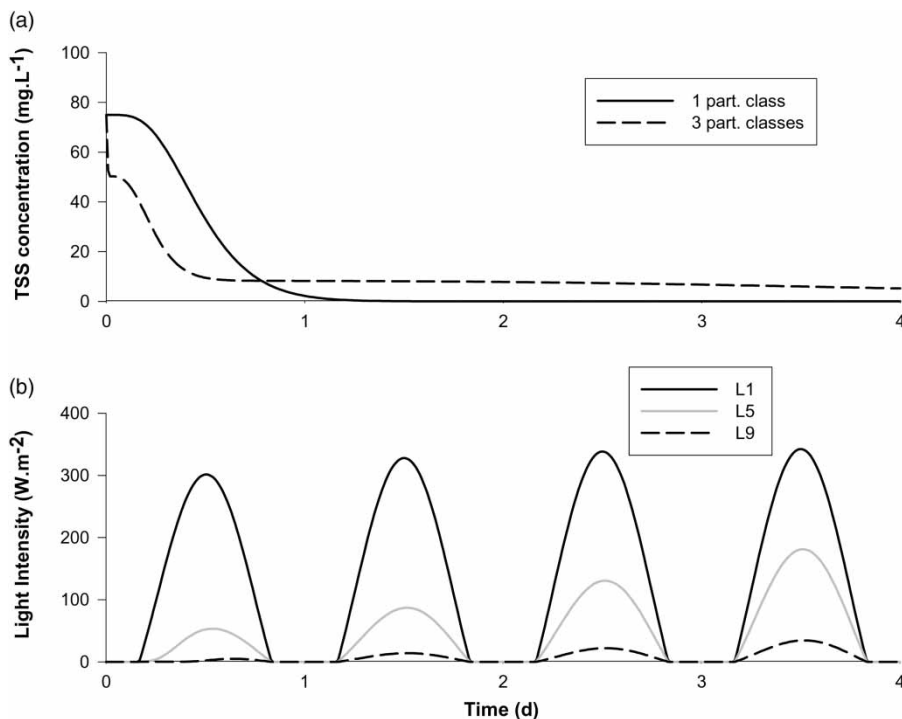
Figure 2 │ Simulation results of the TSS concentration and the light intensity for the simulation with a single and three particle class model. Variables shown are (a) TSS concentration in layer 5 considering a single and three classes of particles, (b) the light intensity in layer 1, 5 and 9 considering three classes of particles.

Figure 3 | Simulation results of the free and attached *E. coli* concentration in layer 5 for the simulation with a single and three particle classes. Parameters shown are (a) free and attached *E. coli* concentration considering a single particle class, (b) free and attached *E. coli* concentration considering three particle classes and (c) total *E. coli* concentration for both simulations.

three particle class (b) model. The results for the single particle class model are extracted from Figure 1. The lower light intensity in subsurface layers for the simulation with three particle classes causes a slower solar disinfection rate for the free *E. coli* (Figure 3(b)). The stepwise decrease of the free *E. coli* concentration during daytime is less important whereas in the simulation with a single particle class (Figure 3(a)) solar disinfection is enhancing the pathogen removal significantly after day 1. For the attached *E. coli* the following phenomena can be seen successively: sorption of *E. coli* to each of the particle classes, settling of *E. coli* attached to the fastest settling particle class ($X_{path,1}$), settling of $X_{path,2}$ and settling of $X_{path,3}$. On Figure 3(b) the total attached *E. coli* concentration in layer 5 is presented as X_{path}. The removal of $X_{path,1}$ accounts for only a small part of the total attached *E. coli* removal because of the ten times lower sorption coefficient (Table 2) and the fast settling velocity of X_1. After one day, the remaining attached *E. coli* is all $X_{path,3}$ for which it takes more than four days to settle out. From the second day, solar disinfection of $X_{path,3}$ can be seen. According to the comparison of Figure 3(a) and (b), the behaviour of X_{path} in the proposed model is very different, considering a single or three particle classes. Given that a single class model is not representative of reality

(Vallet *et al.* 2011), we can conclude from the sensitivity of the results on the number of classes that it is worthwhile to further study the necessary number of classes and their properties (settling velocities, sorption parameters, etc., see Table 2).

In Figure 3(c) the total *E. coli* concentration in layer 5 is presented for both simulations. The simulation with three particle classes presents a slower decrease of total *E. coli*. The main cause for this difference is the difference in solar disinfection. During daytime, the disinfection rate is smaller for the simulation with three particle classes than for the simulation with a single particle class due to the particles remaining in suspension. Thus, in a more realistic stormwater description with a heterogeneous suspension of particles, the removal of *E. coli* is slowed down by a small fraction of slow settling particles, which affect light penetration significantly. In this example, the light extinction coefficient is the same for all the particle classes. However, according to Van Duin *et al.* (2001), the different particle classes have a different impact on the light extinction. The particles with a slow settling velocity will have a stronger impact on the light extinction. In the present case it means that, depending on the concentration of the slowest particles, the disinfection rate could even be smaller than the presented results.

Discussion

The present model has shown the ability to reproduce a heterogeneous suspension of particles and different phenomena affecting pathogens in a stormwater basin as decay, (de)sorption to particles and disinfection by solar radiation. The settling model with layers allows reproduction of the spatial heterogeneity as a function of water depth. It must be stated that no calibration has so far been performed. In that respect it is important that measurements are made of the different pathogen fractions (free and attached) and a study is under way to develop an appropriate protocol. However, the model has been set up with parameters found in the literature and can therefore be used to provide realistic information that supports the development of management strategies for the stormwater basin. For example, on Figure 3 it can be seen that the effect of solar disinfection is dependent on the particle sedimentation velocity distribution and the retention time of the water in the basin. Moreover a small fraction of slow settling particles determines the light penetration and so the solar disinfection of pathogens. In layers closer to the surface, where suspended solids settle out first, solar disinfection becomes more important. This means that the retention of the water in the stormwater basin by introducing valves on the outlet can be an improvement in terms of water quality, especially in shallow stormwater basins. The goal of further work will be to use the pathogens' removal to further optimize the parameters of real-time control rules to optimally manage the stormwater basin (Muschalla *et al.* 2009).

CONCLUSION

This paper has presented a new model to describe the behaviour of pathogens in stormwater basins. Different processes such as base decay, solar disinfection, settling, sorption and desorption to suspended solids have been implemented in a layer model to describe the vertical profiles of light, TSS and free and sorbed pathogens. The dynamics of the concentration of pathogens is well represented for a suspension of particles with different settling velocities, as shown on Figure 3, and the importance of particle settling and solar disinfection are illustrated. This model is easy to use and modify and it accounts for a population of particles characterized by a distribution of different settling velocities. The development of this dynamic population balance model contributes to evaluating the efficiency of introducing real-time control of

valves on stormwater basins that prolong stormwater retention and in this way reduce the load of pathogens to the river.

REFERENCES

Carpenter, J.-F., Vallet, B., Pelletier, G., Lessard, P. & Vanrolleghem, P. A. 2011 Evaluation of the removal efficiency of a retrofitted stormwater detention pond. *J. Environ. Eng.* (submitted).

Chapra, S. C. 1997 *Surface Water-Quality Modeling*. McGraw-Hill, New-York.

Characklis, G. W., Dilts, M. J., Simmons III, O. D., Likirdopulos, C. A., Krometis, L.-A. H. & Sobsey, M. D. 2005 Microbial partitioning to settleable particles in stormwater. *Water Res.* **39**, 1773–1782.

Chebbo, G. & Grommaire, M.-C. 2009 VICAS – an operating protocol to measure the distributions of suspended solid settling velocities within urban drainage samples. *J. Environ. Eng.* **135**, 768–775.

Curtis, T. P., Mara, D. D. & Silva, S. A. 1992 Influence of pH, oxygen, and humic substances on ability of sunlight to damage fecal coliforms in waste stabilization pond water. *Appl. Env. Microbiol.* **58**, 1335–1343.

Fenner, R. A. & Komvuschara, K. 2005 A new kinetic model for ultraviolet disinfection of grey water. *J. Environ. Eng.* **131**, 850–864.

Garcia-Armisen, T. & Servais, P. 2009 Partitioning and fate of particle-associated *E. coli* in river waters. *Wat. Env. Res.* **81**, 21–28.

Guber, A. K., Pachepsky, Y. A., Shelton, D. R. & Yu, O. 2007 Effect of bovine manure on fecal coliform attachment to soil and soil particles of different sizes. *Appl. Env. Microbiol.* **73**, 3363–3370.

Henze, M., Leslie Grady Jr, C. P., Gujer, W., Marais, G. V. R. & Matsuo, T. 1987 A general model for single-sludge wastewater treatment systems. *Water Res.* **21**, 505–515.

Hipsey, M. R., Brookes, J. D., Regel, R. H., Antenucci, J. P. & Burch, M. D. 2006 In situ evidence for the association of total coliforms and *Escherichia coli* with suspended inorganic particles in an australian reservoir. *Water, Air, and Soil Pollution* **170** (1), 191–209.

Jacobsen, B. N. & Arvin, E. 1996 Biodegradation kinetics and fate modelling of pentachlorophenol in bioaugmented activated sludge reactors. *Water Res.* **30**, 1184–1194.

Jeng, H. C., England, A. J. & Bradford, H. B. 2005 Indicator organisms associated with stormwater suspended particles and estuarine sediment. *J. Environ. Sci. Health, Part A: Environ. Sci. Eng. Toxic Hazard. Subst. Control* **40**, 779–791.

Krometis, L. A., Characklis, G. W., Simmons 3rd, O. D., Dilts, M. J., Likirdopulos, C. A. & Sobsey, M. D. 2007 Intra-storm variability in microbial partitioning and microbial loading rates. *Water Res.* **41**, 506–516.

Lindblom, E., Gernaey, K. V., Henze, M. & Mikkelsen, P. S. 2006 Integrated modelling of two xenobiotic organic compounds. *Water Sci. Technol.* **54**, 213–221.

Mancini, J. L. 1978 Numerical estimates of coliform mortality rates under various conditions. *J. Water Pollut. Control Fed.* **50**, 2477–2484.

Muschalla, D., Pelletier, G., Berrouard, É., Carpenter, J.-F., Vallet, B. & Vanrolleghem, P. A. 2009 Ecohydraulic-driven real-time control of stormwater basins. In: *8th International Conference on Urban Drainage Modelling*, Tokyo, Japan, 7–11 September 2009.

Natural Resources Canada 2010 Available from: http://atlas.nrcan.gc.ca/site/english/maps/archives/5thedition/environment/climate/mcr4077/?maxwidth=1600&maxheight=1400&mode=navigator&upperleftx=0&upperlefty=0&lowerrightx= 6784&lowerrighty=5376&mag=0.03125 (accessed 29 September 2010).

Oliver, D. M., Clegg, C. D., Heathwaite, A. L. & Haygarth, P. M. 2007 Preferential attachment of *Escherichia coli* to different particle size fractions of an agricultural grassland soil. *Water Air Soil Pollut.* **185**, 369–375.

Pettersson, T. J. R. 2002 Characteristics of suspended particles in a small stormwater pond. In: *9th International Conference on: Urban Drainage*, Portland, OR, United States, 8–13 September 2002.

Struck, S. D., Selvakumar, A. & Borst, M. 2008 Prediction of effluent quality from retention ponds and constructed wetlands for managing bacterial stressors in storm-water runoff. *J. Irrig. Drainage Eng-ASCE* **134**, 567–578.

Vallet, B., Muschalla, D., Lessard, P. & Vanrolleghem, P. A. 2010 A new dynamic stormwater basin model as a tool for management of urban runoff. In: *7th International Conference on Sustainable Techniques and Strategies in Urban Water Management (Novatech2010)*, Lyon, France, 27 June–1 July 2010.

Vallet, B., Lessard, P. & Vanrolleghem, P. A. 2011 Modelling TSS behaviour in stormwater basins based on fractionation in multiple particle settling velocity classes. *Water Res.* (submitted).

Van Duin, E. H. S., Blom, G., Los, F. J., Maffione, R., Zimmerman, R., Cerco, C. F., Dortch, M. & Best, E. P. H. 2001 Modeling underwater light climate in relation to sedimentation, resuspension, water quality and autotrophic growth. *Hydrobiologia* **444** (1), 25–42.

Vanhooren, H., Meirlaen, J., Amerlinck, Y., Claeys, F., Vangheluwe, H. & Vanrolleghem, P. A. 2003 WEST: modelling biological wastewater treatment. *J. Hydroinform.* **5**, 27–50.

Vaze, J. & Chiew, F. H. S. 2004 Nutrient loads associated with different sediment sizes in urban stormwater and surface pollutants. *J. Environ. Eng.* **130**, 391–396.

Vergeynst, L. 2010 Méthodes pour la mesure et la modélisation d'*Escherichia coli* dans les bassins d'orage (methods for measuring and modelling of *Escherichia coli* in stormwater basin), Faculty of Sciences in Bio-engineering, Ghent University, Gent, Belgium and Département de genie civil et de genie des eaux, Université Laval, Quebec, QC, Canada, p. 154.

Vitasovic, Z. Z. 1989 Continuous settler operation: a dynamic model. In: *Wastewater Engineering* (G. G. Patry & D. Chapman, eds). Dynamic Modelling and Expert Systems. Lewis, Chelsea, MI, pp. 59–81.